STEM CELLS®
CANCER STEM CELLS

Combination of a Ptgs2 Inhibitor and an Epidermal Growth Factor Receptor-Signaling Inhibitor Prevents Tumorigenesis of Oligodendrocyte Lineage-Derived Glioma-Initiating Cells

TAKUICHIRO HIDE,[a,b] TATSUYA TAKEZAKI,[a,b] YUKA NAKATANI,[a] HIDEO NAKAMURA,[b] JUN-ICHI KURATSU,[b] TORU KONDO[a,c]

[a]Laboratory for Cell Lineage Modulation, Center for Developmental Biology, RIKEN, Kobe, Japan; [b]Department of Neurosurgery, Kumamoto University Graduate School of Medical Science, Kumamoto, Japan; [c]Department of Stem Cell Biology, Ehime University Proteo-Medicine Research Center, To-on, Ehime, Japan

Key Words. Neural stem cells • p53 • Glioma • Microarray • Oligodendrocyte precursor cells • HRas • Glioma-initiating cells

ABSTRACT

Recent findings have demonstrated that malignant tumors, including glioblastoma multiforme (GBM), contain cancer-initiating cells (CICs; also known as cancer stem cells), which self-renew and are malignant. However, it remains controversial whether such CICs arise from tissue-specific stem cells, committed precursor cells, or differentiated cells. Here, we sought to examine the origin of the CICs in GBM. We first showed that the overexpression of oncogenic *HRas*^{L61} transformed *p53*-deficient oligodendrocyte precursor cells (OPCs) and neural stem cells (NSCs) into glioma-initiating cell (GIC)-like cells in mice. When as few as 10 of these GIC-like cells were transplanted in vivo, they formed a transplantable GBM with features of human GBM, suggesting that these GIC-like cells were enriched in CICs. DNA microarray analysis showed that widespread genetic reprogramming occurred during the OPCs' transformation: they largely lost their OPC characteristics and acquired NSC ones, including the expression of *prominin1*, *hmga2*, *ptgs2*, and *epiregulin*. In addition, the combination of a Ptgs2 inhibitor and an epidermal growth factor receptor (EGFR)-signaling inhibitor prevented the tumorigenesis of transformed OPCs and human GICs (hGICs) obtained from anaplastic oligodendroglioma, but not of transformed NSCs or hGICs obtained from GBM. Together, these findings suggest that GBM can arise from either OPCs or NSCs and that the therapeutic targets for GBM might be different, depending on each GIC's cell-of-origin. STEM CELLS *2011;29:590–599*

Disclosure of potential conflicts of interest is found at the end of this article.

INTRODUCTION

Cancer-initiating cells (CICs; also referred to as cancer stem cells) self-renew indefinitely and continuously generate the amplifying cancer cells that form the majority of cells in a tumor [1, 2]. It is believed that CICs can arise from normal tissue-specific stem cells, precursor cells, or differentiated cells that have acquired stem cell characteristics as a result of oncogenic mutation. In fact, the overexpression of oncogenes can induce hematopoietic stem/progenitor cells to transform into leukemic stem cell-like cells, which form leukemia when a small number of them are transplanted in vivo [2, 3], suggesting that such induced cancer models can be used to investigate the cell-of-origin for CICs. A number of mutations in oncogenes and tumor-suppressor genes are known to be involved in tumorigenesis; however, except for leukemia, the relationship between the cell-of-origin for CIC and such genetic alterations has not been determined [2, 3].

We and others have shown that specified oligodendrocyte precursor cells (OPCs) and astrocytes can revert to neural stem-like cells that, when cultured under appropriate conditions, can form floating aggregates, express neural stem cell (NSC) markers, and differentiate into neurons as well as glial cells [4–7], suggesting that OPCs and astrocytes, as well as NSCs, can serve as the cell-of-origin for brain CICs.

Among a number of mutations associated with gliomagenesis, p53 is the most frequently mutated tumor-suppressor gene in human glioblastoma multiforme (GBM) [8–11], and increased activation of the Ras-signaling pathway is also found in human gliomas, including about 90% of GBM cases [10–12]. Moreover, the deletion of both p53 and NF1, which negatively regulates the Ras-signaling pathway, causes malignant gliomas in mice [13, 14]. Together, these findings led us to examine whether the combination of p53 deletion and Ras activation can induce cultured NSCs, OPCs, and astrocytes to transform into glioma-initiating cell (GIC)-like cells.

Author contributions: T.H.: conception and design, data collection, data analysis and interpretation, manuscript writing; T.T.: data collection, data analysis and interpretation; Y.N.: data collection and analysis; H.N.: provision of study material; J.-I.K.: financial support, provision of study material; T.K.: conception and design, data analysis and interpretation, manuscript writing, financial support, final approval of manuscript.

Correspondence: Toru Kondo, Ph.D., Department of Stem Cell Biology, Ehime University Proteo-Medicine Research Center, Shitsukawa, To-on, Ehime 791-0295, Japan. Telephone: 81-89-960-5925; Fax: 81-89-960-5927; e-mail: tkondo@m.ehime-u.ac.jp Received June 1, 2009; accepted for publication January 26, 2011; first published online in STEM CELLS *EXPRESS* February 25, 2011. 1066-5099/2009/$30.00/0 doi: 10.1002/stem.618

Materials and Methods

Animals and Chemicals

Mice were obtained from the Laboratory for Animal Resources and Genetic Engineering at the RIKEN Center for Developmental Biology (CDB) and from Charles River Japan, Inc. All mouse experiments were performed following protocols approved by the RIKEN CDB Animal Care and Use Committee. Genotyping of *p53*-knockout mice was done by polymerase chain reaction (PCR) as described previously [15]. Chemicals and growth factors were purchased from Sigma-Aldrich (St. Louis, MO, www.sigmaaldrich.com) and Peprotech (Rocky Hill, NJ, www.peprotechec.com), respectively, except where indicated.

Cell Culture

NSCs were prepared from embryonic day 13.5 *p53*-deficient mouse telencephalon and expanded as described previously [16]. For immunostaining, neurospheres were cultured on poly-D-lysine (15 μg/ml)-coated and fibronectin (1 μg/ml, Invitrogen, Carlsbad, CA, www.invitrogen.com)-coated eight-well chamber slides (Nalge Nunc, Rochester, NY, www.nalgenunc.com) in the presence of basic fibroblast growth factor (bFGF; 10 ng/ml) and epidermal growth factor (EGF; 10 ng/ml) for up to 1 day. Astrocyte differentiation was induced in NSC cultures by changing the medium to Dulbecco's modified Eagle's medium (DMEM; Nacalai Tesque, Kyoto, Japan, www.nacalai.co.jp/global) with 10% fetal calf serum (FCS) for three weeks. OPC differentiation was induced by culturing NSCs in DMEM containing platelet-derived growth factor AA (10 ng/ml), bFGF (2 ng/ml), and 0.25% FCS (OPC medium) and purified by sequential immunopanning, as described previously [17]. The human oligodendroglioma cell line Hs683 and GBM line U251, both of which were purchased from ATCC (Manassas, VA, www.atcc.org), were cultured in DMEM supplemented with 10% FCS, 100 units/ml penicillin G, and 100 μg/ml streptomycin (Nacalai Tesque, Japan).

Transfection

Transfection of NSCs, astrocytes, OPCs, and human GICs (hGICs) was performed using the Nucleofector procedure, according to the supplier's instructions (Lonza, Cologne, Germany, www.lonzabio.com). In brief, 2×10^6 cells were suspended in the mouse NSC nucleofector solution (100 μl) with 10 μg vectors, and then were transfected using the nucleofector device. Transfected cells were cultured in their optimized medium.

Immunostaining

Immunostaining was carried out as described previously [17]. The following antibodies were used to detect antigens: mouse anti-glial fibrillary acidic protein (GFAP; 1:500; Millipore, Billerica, MA, www.millipore.com, 1:400; Sigma for human cells), rat anti-Nestin (1:1,000; BD Pharmingen, Franklin Lakes, NJ, 1:200; Millipore for human cells), mouse anti-MAP2(a+b) (1:200; Abcam, Cambridge, MA, www.abcam.com), mouse anti-beta tubulin isotype III (1:400; Sigma for human cells), mouse A2B5 (1:2; hybridoma supernatant; ATCC), mouse anti-galactocerebroside (GC; 1:2; hybridoma supernatant; ATCC), rat anti–green fluorescence protein (anti-GFP; 1:1,000; Nacalai Tesque), rabbit anti-prominin1 (1:100; Abcam), and rabbit anti-human CD133 (1:50; Abcam). The antibodies were detected with goat anti-rat IgG-A488 (1:400; Invitrogen), goat anti-mouse IgG-Cy3 (1:400; Jackson ImmunoResearch, West Grove, PA, www.jacksonimmuno.com), goat anti-rabbit IgG-Cy3 (1:400; Jackson ImmunoResearch), goat anti-mouse IgG-A488 (1:400; Invitrogen), and goat anti-mouse IgM-Texas Red (1:400; Jackson ImmunoResearch). To visualize nuclei, the cells were counterstained with 4′,6-diamidino-2-phenylindole (1 μg/ml).

Paraffin-embedded tumors were sectioned at 6-μm thickness. Antigens were retrieved by HistoVT One according to the supplier's instructions (Nacalai Tesque). Endogenous peroxidase activity was inactivated by applying 0.3% H_2O_2 for 15 minutes at room temperature (RT). The sections were then pretreated with blocking solution (2% skim milk, 0.3% Triton X-100, phosphate-buffered saline [PBS]) for 30 minutes at RT, and incubated with mouse anti-epidermal growth factor receptor vIII (EGFRvIII) antibody clone DH8.3 (1:20, Novocastra) for 30 minutes at RT. The antibodies were visualized with the Vectastain ABC kit (Vector Laboratories, Burlingame, CA, www.vectorlabs.com) and diaminobenzidine (Vector Laboratories).

Proliferation Assay

Two thousand cells were cultured in 100 μl of culture medium in each well of 96-well plates. To examine cell proliferation, the 3-(4,5-di-methylthiazol-2-yl)-2,5-diphenyltetrazolium bromide (MTT) assay was performed as follows. Ten microliters of MTT (5 mg/ml, Nacalai Tesque) was added to each well on days 0, 2 or 3, and 4 in vitro. The cells were incubated for 4 hours, the medium was replaced with 100 μl of DMSO, the cells were dissociated, and cell proliferation was quantified on a Benchmark microplate reader (Bio-Rad, Hercules, CA, www.bio-rad.com) with the absorption spectrum at 570 nm.

Soft Agar Assay

A soft agar assay was performed to examine whether the transfected cells could proliferate anchorage independently. The transfected cells were suspended in 0.3% top agar made with the optimized medium and layered onto 0.6% bottom agar made with the same medium. After the top agar had polymerized, culture medium was added, and the cells were cultured for 20 days with medium changes every three days.

Reverse Transcription Polymerase Chain Reaction (RT-PCR)

RT-PCR was carried out as described [4]. Dimethylsulfoxide (DMSO) or Betaine was added to the reaction mixture for *olig1* (5% DMSO), *olig2* (5% DMSO), *contactin1* (5% DMSO), *sox2* (*10%* DMSO), *nestin* (5% DMSO), and *egfr variant III* (*egfrvIII*) (0.5 M Betaine). Cycle parameters were 20 seconds at 94°C, 40 seconds at 58°C, and 45 second at 72°C for 35 cycles. For *gapdh*, they were 15 seconds at 94°C, 30 seconds at 53°C, and 90 seconds at 72°C for 22 cycles.

The following oligonucleotide DNA primers were synthesized. For exogenous *hras*, the 5′ primer was 5′-ATGACA GAATACAAGCTTGTGGTG-3′, and the 3′ primer was 5′-ATTAACCCTCACTAAAGGGAAG-3′. For *amphiregulin* (*areg*), the 5′ primer was 5′-ATTCAGTCAGAGTTGAA CAGGT-3′, and the 3′ primer was 5′-ACTTTTCTCCA CACCGTTCACC-3′. For *nephroblastoma overexpressed gene* (*nov*), the 5′ primer was 5′-GCATTAACTGCATTGAGCA GAC-3′, and the 3′ primer was 5′-TCTTGGAGGAAGGCCT CATTG-3′. For *prominin1* (*prom1*), the 5′ primer was 5′-AGGCTACTTTGAACATTATCTGCA-3′, and the 3′ primer was 5′-GGCTTGTCATAACAGGATTGT-3′. For *twist homolog 2* (*twist2*), the 5′ primer was 5′-ATGGAGGAGGGCTC CAGCTC-3′, and the 3′ primer was 5′-CTAGTGGGAGGCG GACATGG-3′. For *Kruppel-like factor 4* (*klf4*), the 5′ primer was 5′-CACATGAAGCGACTTCCCCC-3′, and the 3′ primer

was 5′-TTGATGTCCGCCAGGTTGAAG-3′. For *muscle-blind-like 3* (*mbnl3*), the 5′ primer was 5′-CTGTGACAA TCTGCATGGATTAC-3′, and the 3′ primer was 5′-TTG CCTGTAGTTGTTGGAACGTA-3′. For *S100 calcium binding protein A6* (*s100a6*), the 5′ primer was 5′-ATGG CATGCCCTCTGGATCAG-3′, and the 3′ primer was 5′-TTATTTCAGAGCTTCATTGTAGATC-3′. For *paired related homeobox 1* (*prrx1*), the 5′ primer was 5′-CAGGCCTTG GAGCGTGTCTT-3′, and the 3′ primer was 5′-TCAGTT GACTGTTGGCACCTG-3′. For *high mobility group AT-hook 2* (*hmga2*), the 5′ primer was 5′-ATGAGCGCAC GCGGTGAGGG-3′, and the 3′ primer was 5′-CTAATC CTCCTCTGCGGACTC-3′. For *prostaglandin-endoperoxide synthase 2* (*ptgs2*), the 5′ primer was 5′-CATTCTTTGCC CAGCACTTCA-3′, and the 3′ primer was 5′-GTGGCATA CATCATCAGACCA-3′. For *contactin1*, the 5′ primer was 5′-GTCACCAGCCAGGAGTACTC-3′, and the 3′ primer was 5′-CAGGAGCAAGCTGAGGAGAC-3′. For *NK2 homeobox 2* (*nkx2.2*), the 5′ primer was 5′-ATGTCGCT-GACCAACA CAAAGA-3′, and the 3′ primer was 5′-TCAC-CAAGTC CACTGCTGGGCCTG-3′. For *myelin basic protein* (*mbp*), the 5′ primer was 5′-ATGGCATCACAGAAGA-GACCCT-3′, and the 3′ primer was 5′-CTGTCTCTTCCTCCCAGCTTAAA-3′. For *proteolipid protein* (*plp*), the 5′ primer was 5′-GACAAGTTTGTGGGCAT-CACC-3′, and the 3′ primer was 5′-TCGGCCCATGAGTT-TAAGGAC-3′. For *lipoma HMGIC fusion partner-like 3* (*lhfpl3*), the 5′ primer was 5′-GCTCTTCCACTACTG-CATCGG-3′, and the 3′ primer was 5′-ATTCCGATGA-TAGCCAGGATGT-3′. For *breast carcinoma amplified sequence 1* (*bcas1*), the 5′ primer was 5′-GAAAGACTC-CAGCTGCCAAAC-3′, and the 3′ primer was 5′-ATCCGCTTTGGTCCCAGGCC-3′. For *G0/G1switch 2* (*g0s2*), the 5′ primer was 5′-CCTGGCCAAGGAGAT-GATGGC-3′, and the 3′ primer was 5′-CTAGGAG-GCGTGCTGCCGG-3′. For *protein phosphatase 2* (formerly *2A*), *regulatory subunit B, beta* (*ppp2r2b*), the 5′ primer was 5′-TTCAGCCACAGTGGGAGGTA-3′, and the 3′ primer was 5′-TTTGCTAAAGTCCAGACTGTC-3′. For *nucleosome assembly protein 1-like 5* (*nap1l5*), the mouse 5′ primer was 5′-ATGGCCGACCCCGAGAAGCAG-3′, the human 5′ primer was 5′- ATGGCCGACTCGGAAAACCA-3′, and the 3′ primer was 5′-GAGCTCTTGGATCTTGGCGAG-3′. For *heparin-binding EGF-like growth factor* (*hbegf*), the mouse 5′ primer was 5′- CTTTCTCCTCCAAGCCACAAG-3′, and the 3′ primer was 5′- CCATGCCCAACTTCACTTTCTC-3′. For *epiregulin* (*ereg*), the mouse 5′ primer was 5′- CATCTAC CTGGTGGACATGAG-3′, and the 3′ primer was 5′- CTG AGGTCACTCTCTCATATTC-3′. For *egfr*, the mouse 5′ primer was 5′- GATGAAAGAATGCATTTGCCAAG-3′, and the 3′ primer was 5′- GGGGCTGATTGTGATAGACAGG-3′. For *egfrvIII*, the mouse 5′ primer was 5′-ATGCGACCCT CCGGGACGG-3′, and the 3′ primer was 5′-ATTCCGTTA CACACTTTGCGGC-3′. The primers for *nestin*, *musashi1*, *sox2*, *olig1*, *olig2*, *mash1*, and *gapdh* were described previously [16].

Microarray Hybridization and Data Processing

Five micrograms of total RNA were labeled with biotin by in vitro transcription using the One-Cycle Target Labeling procedure (Affymetrix, Santa Clara, CA, www.affymetrix.com). The cRNA was subsequently fragmented and hybridized to the GeneChip Mouse Genome 430 2.0 array (Affymetrix), according to the manufacturer's instructions. The microarray image data were processed with the GeneChip Scanner 3000 (Affymetrix) to generate cell library (CEL) data. The CEL data were then subjected to analysis with the dChip software [18], which can normalize and process multiple datasets simultaneously. Data were normalized within the respective groups, according to the program's default setting. Statistical significance was determined by the eBayes method [19] and by ANOVA for two- and three-sample comparisons, respectively. The q value, which is an extension of a quantity called the "false discovery rate (FDR)," was examined to evaluate the genome-wide tests of significance [20, 21]. FDR < 0.1.

Human Brain Tumors

Eleven GBMs, five anaplastic astrocytomas, five anaplastic oligodendrogliomas (AOs), three anaplastic oligoastrocytomas, and two hGICs, hGIC1 and hGIC2, were used following the research guidelines of the RIKEN Center for Developmental Biology and Kumamoto University Graduate School of Medical Science. The detailed characterization of the hGICs will be reported elsewhere (T.T and T.K., unpublished data). Poly(A)+ RNA was prepared from glioma spheres using a QuickPrep mRNA Purification Kit (GE Healthcare, Little Chalfont, U.K., www.gehealthcare.com). Human control brain total RNA was purchased from Invitrogen. The cDNAs were synthesized using a Transcription First Strand cDNA Synthesis Kit (Roche, Basel, Switzerland, http://www.roche.com).

Flow Cytometry

Cells transfected with vectors or immunolabeled for Prom1 (1:200; Abcam) were analyzed in a JSAN cell sorter (Bay Bioscience, Kobe, Japan, www.baybio.co.jp) using dual-wavelength analysis (488 nm solid-state laser and 638-nm-semiconductor laser). Propidium iodide-positive (i.e., dead) cells were excluded from the analysis.

Vector Construction

Full-length mouse *HRas* was amplified from mouse NSC cDNA using RT-PCR and Phusion polymerase (Finnzymes, Espoo, Finland), according to the manufacturer's instructions, and was cloned into a pDrive vector (Qiagen, Venlo, Netherlands, www.qiagen.com). $HRas^{L61}$ was made by replacing the glycine at codon 61 with leucine, by PCR. The nucleotide sequences were verified using the BigDye Terminator Kit version 3.1 (Applied Biosystems, Foster City, CA, www.appliedbiosystems.com) and ABI sequencer model 3130xl (Applied Biosystems). $HRas^{L61}$ cDNA was inserted into the pCMS-EGFP vector, resulting in pCMS-EGFP-HRasL61.

The following oligonucleotide DNAs were synthesized. For the full-length mouse *HRas*, the 5′ primer was 5′-TGAATTCGCCACCATGACAGAATACAAGCTTGTGGTG-3′ and the 3′ primer was 5′-ACTCGAGTCAGGACAGCACA-CATTTGCAG-3′. For $HRas^{L61}$, the 5′ primer was 5′-ACAG-CAGGTCTAGAAGAGTATA-3′ and the 3′ primer was 5′-TATACTCTTCTAGACCTGCTGT-3′.

Intracranial Cell Transplantation into the Brain of Nude Mice

Control cells and transfected cells were suspended in 5 μl of culture medium and injected into the brain of 5- to 8-week-old female nude mice that had been anesthetized with 10% pentobarbital. The stereotactic coordinates of the injection site were 2-mm forward from lambda, 2-mm lateral from the sagittal suture, and 5-mm deep.

Brain Fixation and Histopathology

The dissected mouse brains were fixed in 4% paraformaldehyde at 4°C overnight. After fixation, the brains were cryoprotected with 12%–18% sucrose in PBS and embedded in Tissue-Tek OCT compound (Miles, Elkhart, IN). Coronal

sections (10-μm thick) were prepared from the cerebral cortex and stained with H&E using a standard technique.

Oral Administration of Drugs to Mice That Had Been Injected with Transformed Cells

The EGFR-signaling inhibitor, Gefitinib (200 mg/kg/day; AstraZeneca, London, U.K., www.astrazeneca.com), and Ptgs2 inhibitor, celecoxib (60 mg/kg/day; Astellas, Tokyo, Japan, www.astellas.com), were orally administered every day after the operation, using a disposable flexible-type animal-feeding needle (Fuchigami, Kyoto, Japan).

Statistical Analysis

The survival data were analyzed for significance by Kaplan-Meier methods using GraphPad Prism version 4 software (p values were calculated with the log-rank test, GraphPad Software, La Jolla, CA, www.graphpad.com).

Results

The Combination of Ras Activation and p53 Deletion Transforms NSCs and OPCs, but Not astrocytes, into GIC-like Cells

We prepared NSCs, astrocytes, and OPCs as described previously [22–24]. Over 95% of the NSCs, 98% of the astrocytes, and 95% of the OPCs were positive for their respective specific markers, Nestin, GFAP, and A2B5 (Fig. 1A, 1B). We transfected these cell populations with either a control vector or a $HRas^{L61}$ expression vector [25], and established cell lines (NSC-C, AST-C, OPC-C, NSC-L61, AST-L61, and OPC-L61), which maintained their original marker immunoreactivities, although the transfected astrocytes lost their GFAP immunoreactivity during culture, as described previously [9] (Fig. 1C, 1D). We first examined whether Ras activation could induce the transformation of NSCs, astrocytes, or OPCs. Both NSC-L61 and OPC-L61 formed colonies in soft agar, whereas AST-L61 did not, although Ras activation significantly accelerated the proliferation of all the transfected lines, determined by the MTT assay (Fig. 1E–1J). These data suggest that the combination of Ras activation and p53 deletion transforms NSCs and OPCs but not astrocytes.

To investigate the tumor-forming ability of the transfected cells, we injected 1,000 cells of each type into the brain of nude mice. Mice that received either NSC-L61 (n = 10 of 10) or OPC-L61 (n = 9 of 9) developed brain tumors and died within 30 days, whereas none that were given injections of 10^3 AST-L61 (n = 10), or 10^5 control NSC-C (n = 3), AST-C (n = 3), or OPC-C (n = 3) showed evidence of brain tumorigenesis (Fig. 2A–2C). Although tumors that had characteristics of human astrocytoma, including hypercellularity and pleomorphism, formed in three of eight mice injected with 10^4 AST-L61 cells (Fig. 3), the secondary transplantation of 10^4 GFP+ cells did not result in brain tumors, suggesting that AST-L61 does not contain bona fide GIC-like cells or that AST-L61 cells need an additional mutation(s) to transform into GICs.

We further examined the tumorigenic ability of NSC-L61 and OPC-L61. Five of seven mice injected with 100 NSC-L61 cells and three of six mice injected with 10 NSC-L61 cells formed brain tumors (Fig. 2A). In the case of OPC-L61, all of the mice (5/5) injected with 100 cells and three of four mice injected with 10 cells developed brain tumors and died (Fig. 2B). These results suggest that both NSC-L61 and OPC-L61 were highly enriched in GIC-like cells.

NSC-L61 and OPC-L61 Cells Form Transplantable GBM with Features of Human GBM

We next examined the histopathology of the brain tumors formed from NSC-L61 and OPC-L61 (Fig. 2D–2K), to determine their type. The tumors were composed of GFP^+ cells, many of which were invading the adjacent brain tissue (Fig. 2D, 2H). H&E staining revealed that the tumors had characteristics of human GBM, including hypercellularity, pleomorphism, multinuclear giant cells, mitosis, and necrosis [26] (Fig. 2E–2G, 2I–2K). To characterize the tumors further, we acutely immunolabeled the dissociated tumor cells for both GFP and neural markers, and found that the tumor-forming cells maintained their original immunoreactivity (Supporting Information Fig. 1).

We then performed serial transplantation experiments using cells from the tumors that had formed in mice injected with either 100 NSC-L61 or 100 OPC-L61 cells. Within four weeks, all of the mice (n = 10 each for NSC-L61- and OPC-L61-derived tumors) that received secondary transplantation developed brain tumors that recapitulated the phenocopy of the primary transplantation (Fig. 2L–2O), indicating that NSC-L61 and OPC-L61 had a high capacity for self-renewal. Moreover, we found that 76% of the NSC-L61 and 44% of the OPC-L61 cells were positive for Prominin1 (Prom1), a putative marker for brain CICs [27, 28] and NSCs [29], whereas only 3% of the control NSCs and 4% of the OPCs were positive for Prom1 (Supporting Information Fig. 2). These data collectively suggest that a significant proportion of both NSC-L61 and OPC-L61 cells are transformed into GIC-like cells.

OPC-L61 Acquired the Expression of NSC-Specific Genes and Extensively Lost the Expression of OPC-Specific Genes

We used gene expression profiling to characterize the changes in gene expression that occurred during the transformation of NSCs and OPCs. We found that the gene expression profile of OPC-L61 was similar to that of control NSC-C and NSC-L61 but different from that of OPC-C (Fig. 4A–4C). A group of genes that were highly expressed in OPC-C showed decreased expression in OPC-L61 and vice versa, suggesting that the OPCs underwent global reprogramming of their gene expression during their transformation to OPC-L61.We then used RT-PCR to assess whether OPC-L61 acquired the expression of NSC-specific genes and lost that of OPC-specific genes (Fig. 4D, 4E). Tissue-specific stem cell markers, including *prom1*, *hmga2*, and *nov*, were expressed in OPC-L61 but not OPC-C, whereas the expression of several OPC-specific genes, *contactin1*, *olig1*, *olig2*, *mbp*, and *plp*, significantly decreased in OPC-L61. Moreover, a number of genes, including *twist2*, *klf4*, *mbnl3*, *s100a6*, *prrx1*, *ptgs2*, and *ereg*, were predominantly expressed in OPC-L61, NSC-C, and NSC-L61, whereas *lhfpl3*, *bcas1*, *g0s2*, *ppp2r2b*, and *nap1l5*, all of which were expressed in OPC-C, decreased in OPC-L61. Together, these data suggest that during transformation, the gene expression profile of OPCs changes markedly, and becomes similar to that of NSCs.

The Combination of a Ptgs2 Inhibitor and an EGFR-Signaling Inhibitor Prevents the Tumorigenicity of OPC-Derived GIC-Like Cells and Oligodendroglioma-Derived GICs

The finding that OPCs acquired characteristics of NSCs when transformed into GIC-like cells led us to examine whether the upregulated genes in the GIC-like cells include therapeutic targets. Among the candidate genes, we focused on Ptgs2 and

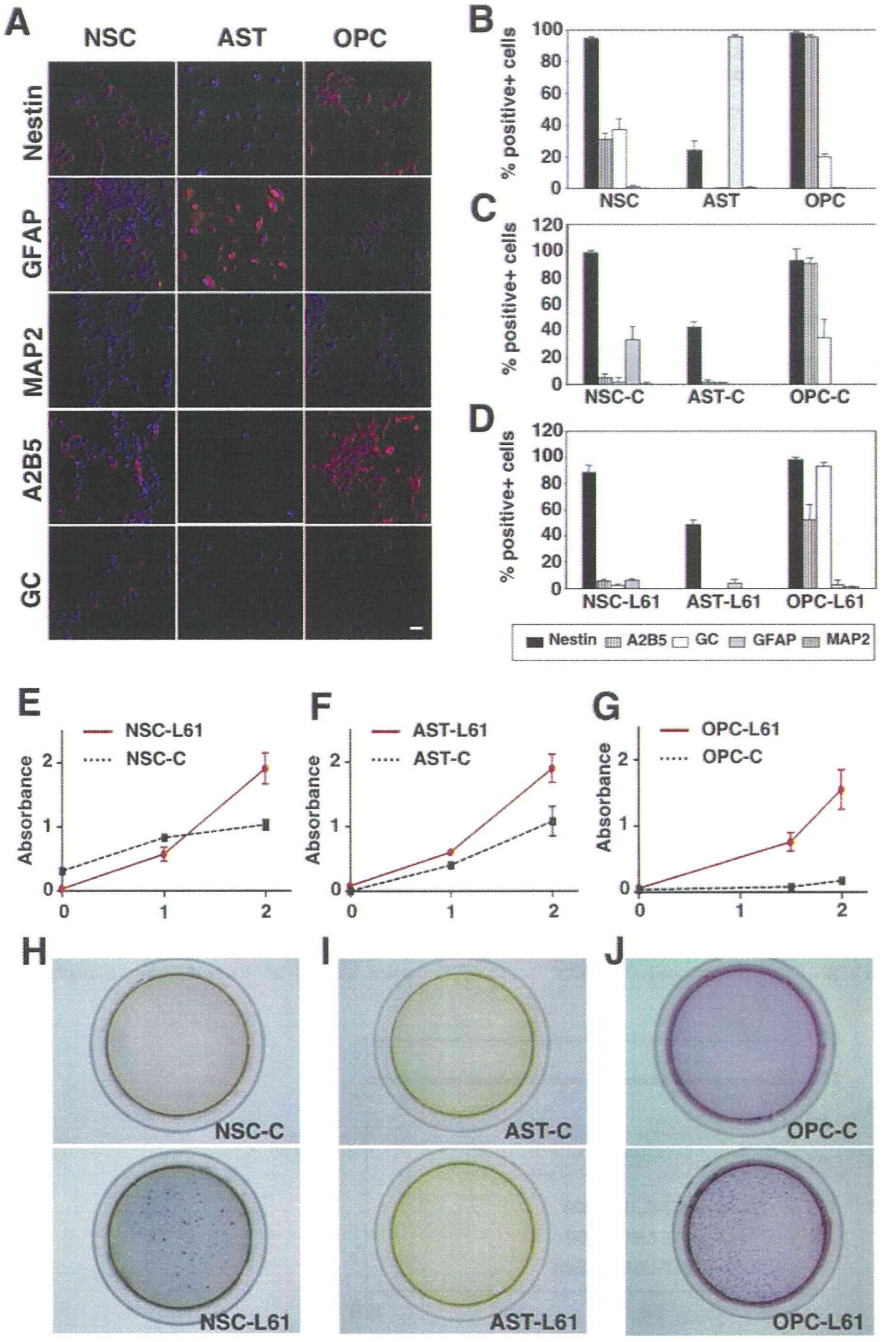

Figure 1. Characterization of $HRas^{L61}$-transfected *p53*-deficient NSCs, ASTs, and OPCs. **(A):** *p53*-deficient NSCs, ASTs, and OPCs immunolabeled for neural lineage markers (red) and 4′,6-diamidino-2-phenylindole (blue). Scale bar = 15 μm. **(B–D):** Proportion of neural lineage marker-positive cells in untransfected cells, NSCs, ASTs, and OPCs **(B)**, control vector-transfected cells NSC-C, AST-C, and OPC-C **(C)**, and $HRas^{L61}$ vector-transfected cells NSC-L61, AST-L61, and OPC-L61 **(D)**, are shown as the mean ± SD of three cultures. **(E–G):** Proliferation of untransfected (dotted black line) and $HRas^{L61}$ vector-transfected (red line) cells, determined using the 3-(4,5-di-methylthiazol-2-yl)-2,5-diphenyltetrazolium bromide assay. Results shown are the mean ± SD of three cultures. **(H–J):** NSC-L61 **(H)** and OPC-L61 **(I)**, but not AST-L61 **(J)**, formed colonies in soft agar. Abbreviations: AST, astrocyte; GC, galactocerebroside; GFAP, glial fibrillary acidic protein; MAP2, microtubule associated protein 2; NSC, neural stem cell; OPC, oligodendrocyte precursor cell.

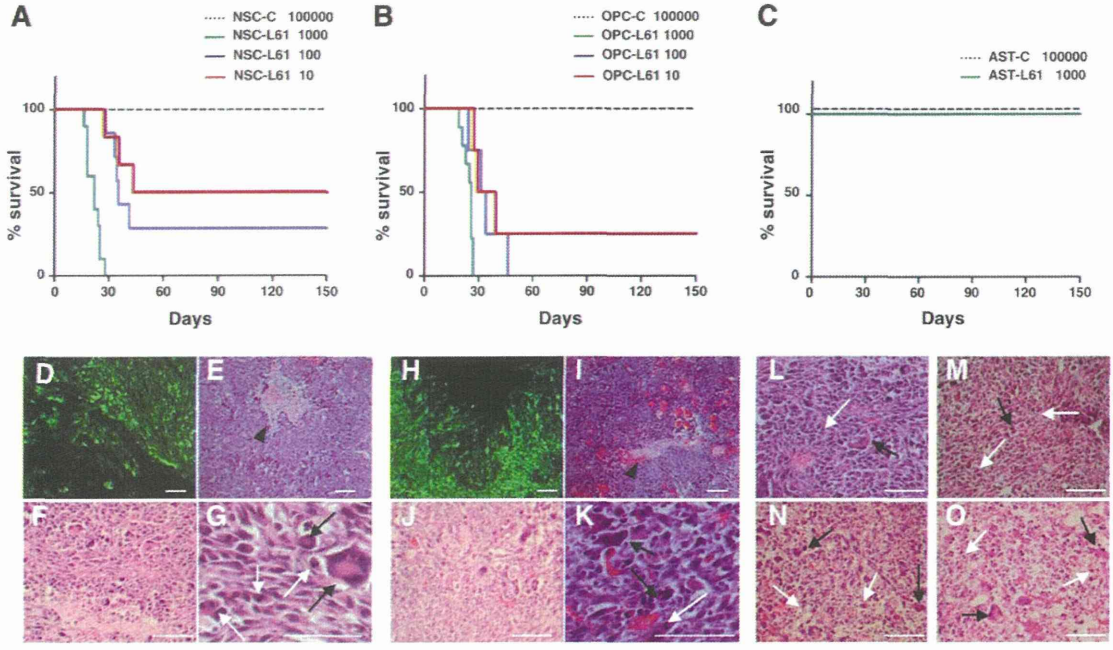

Figure 2. NSC-L61 and OPC-L61, but not AST-L61, are enriched in glioma-initiating cell-like cells. **(A–C):** Survival curves for mice injected with a limiting dilution of NSC-L61 **(A)**, OPC-L61 **(B)**, and AST-L61 **(C)**. **(D–O):** Brain sections with tumors derived from NSC-L61 **(D–G)** and OPC-L61s **(H–K)**. Both types of transformed cells invaded the brain parenchyma (green in **[D, H]**). H&E staining of the tumors showed necrosis (arrowhead in **[E, I]**), hypercellularity and hypervascularity, multinuclear giant cells (black arrow), and mitotic cells (white arrow) **(G, K)**; these pathological features are similar to human glioblastoma multiforme. H&E staining of secondary tumors **(M, O)** showed they were phenocopies of the primary tumors **(L, N)**. Scale bar = 100 μm. Abbreviations: AST, astrocyte; NSC, neural stem cell; OPC, oligodendrocyte precursor cell.

factors in the epidermal growth factor (EGF)-signaling pathway, because *ptgs2*, *egf receptor* (*egfr*), and various types of EGFR ligands, are highly expressed in human gliomas and other cancers and are involved in tumor progression [30, 31]. Indeed, we found that the OPC-L61 and NSC-L61 cells expressed *egfr* and EGFR ligands *areg*, *hbegf*, *ptgs2*, and *ereg* (Fig. 5A).

To evaluate the expression of *ptgs2*, EGFR ligands, and *egfr* in GICs, we established two hGIC lines, hGIC1 and hGIC2, from primary AO and GBM tissues, respectively, as shown previously [26, 27, 32]. Both of the hGIC lines formed transplantable malignant gliomas in the brains of nude mice when as few as 10 cells were transplanted, suggesting that

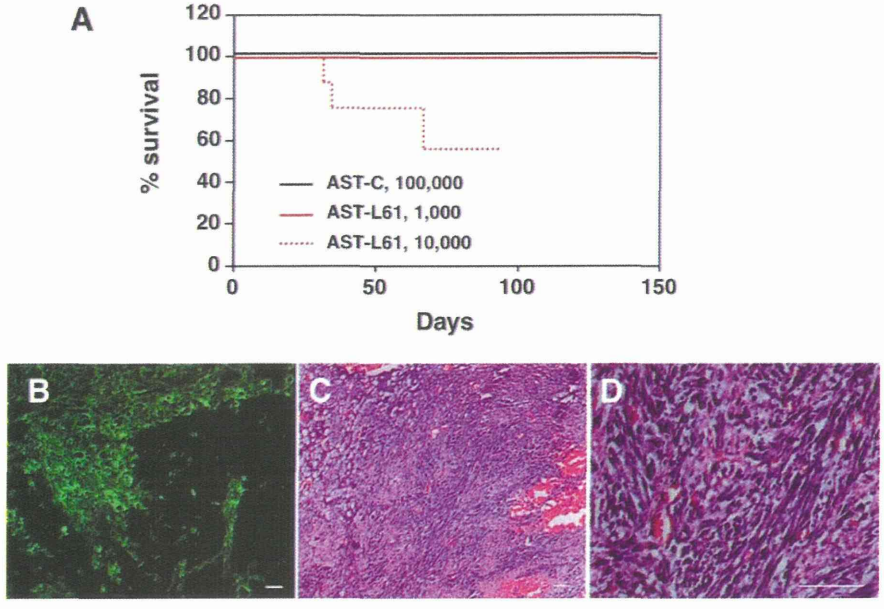

Figure 3. Pathological features of tumors formed by AST-L61. **(A):** Survival curves for mice injected with control astrocytes (AST-C) or AST-L61. **(B):** AST-L61 cells invaded the brain parenchyma (green). **(C, D):** H&E staining of the tumors showed a monotonous fibrous morphology with neither necrosis nor multinucleic giant cells. Scale bar = 100 μm. Abbreviation: AST, astrocyte.

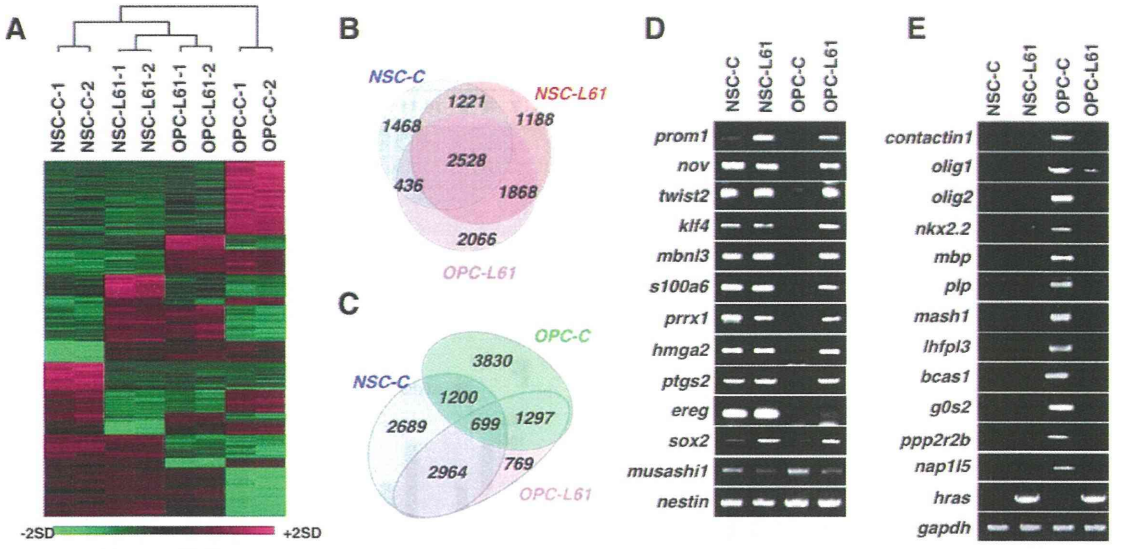

Figure 4. Evidence of global changes in gene expression in OPC transformation. **(A):** Hierarchical clustering using the Affymetrix murine 430A 2.0 microarray demonstrated that OPC-L61 exhibited a gene expression profile most similar to NSC-L61. **(B, C):** Diagram of the number of genes that were expressed specifically or commonly in NSC-C, OPC-C, NSC-L61, and OPC-L61. **(D, E):** Expression analysis of NSC-specific genes **(D)** and OPC-specific genes **(E)** in NSC-C, NSC-L61, OPC-C, and OPC-L61 by reverse transcription polymerase chain reaction. *gapdh* expression was an internal control. Abbreviations: NSC, neural stem cell; OPC, oligodendrocyte precursor cell.

these lines were also enriched in CICs (T.T. and T.K., unpublished observation). We confirmed that the hGICs expressed *ptgs2* and EGFR ligands, whose expression was undetectable in normal brain samples (Fig. 5B). We also found that hGIC1 expressed *egfr* version III (*egfrvIII*), a constitutively active form of EGFR that is expressed in malignant glioma, and *egfr*, whereas hGIC2 expressed *egfr* only. Moreover, we confirmed the expression of *egfrvIII* in the human AO and GBM sections and in paraffin-embedded hGIC xenografts by immunohistochemical analysis, as shown previously (Supporting Information Fig. 3) [33]. We further found that *ptgs2* and EGFR ligands were predominantly expressed in malignant human gliomas and that 5 of 11 GBM, 2 of 5 AO, and an oligodendroglioma cell line Hs683 expressed *egfrvIII* (Fig. 5C; Supporting Information Fig. 4). Together, these data suggest that both *Ptgs2* and EGFR-signaling pathways are involved in GIC functions.

Inhibitors for Ptgs2 and the EGFR-signaling pathways are used separately as chemotherapeutic reagents for lung cancer, intestinal neoplasm, non-small cell lung carcinoma, and glioma in human. As their use in combination has been shown to block tumorigenesis in both $APC^{Min/+}$ mice [34] and head-and-neck carcinoma xenografted mice [35], but has not been examined for GBM, we tested the efficacy of their combination in NSC-L61, OPC-L61, hGIC1, and hGIC2. Gefitinib, an EGFR inhibitor, and Celecoxib, a Ptgs2 inhibitor, prevented the proliferation of NSC-L61, OPC-L61, and hGIC cells in a dose-dependent manner, and the combination had additive effects, although control NSCs and OPCs were also affected (Fig. 5D–5G).

We next addressed whether this drug combination blocks the tumorigenesis of NSC-L61, OPC-L61, or hGICs in vivo, as neither Gefitinib nor Celecoxib alone showed any effect on the survival time of NSC-L61- (data not shown), OPC-L61-, or hGIC1-injected mice (Supporting Information Fig. 5). The mean survival time of mice injected with OPC-L61 was significantly longer in the drug-treated group (34.1 ± 9.5 days, $p = .005$), compared with control (23.0 ± 1.9 days), whereas the combination had little effect on mice injected with NSC-L61 (21.0 ± 2.9 days in drug-treated vs. 19.7 ± 6.9 days in control; Fig. 5H, 5I). In addition, the mean survival time of mice injected with hGIC1 was longer in the drug-treated group (56.2 ± 8.2 days, $p = .0027$), compared with control mice (44.5 ± 3.4 days), whereas the combination did not increase the mean survival time of mice injected with hGIC2 (37.6 ± 1.1 days in drug-treated vs. 34.6 ± 2.6 days in control; Fig. 5J, 5K). We confirmed that the drug combination could block the tumorigenesis of an oligodendroglioma cell line, Hs683, but not of a GBM line, U251 (Supporting Information Fig. 4). In addition, we found that the knockdown of both *egfr* and *ptgs2* inhibited the proliferation of OPCL61 and hGIC1 cells but not of NSCL61 and hGIC2 cells (data not shown). Together, these results suggest that both EGFR and Ptgs2 are crucial for the proliferation of oligodendrocyte lineage-derived malignant glioma, and that a drug combination targeting both pathways specifically prevents its tumorigenesis.

Discussion

Here, we demonstrated that a combination of oncogenic $HRas^{L61}$ overexpression and *p53* deletion, both of whose pathways are frequently mutated in human GBM [8–12], transformed NSCs and OPCs into GIC-like cells. The injection of only 10 of these GIC-like cells formed transplantable GBM with characteristics of human GBM in the brain of nude mice, suggesting that these cells are enriched in CICs and that both NSCs and OPCs are likely cells-of-origin for GBM. In contrast, we found that the same combination could not transform astrocytes; AST-L61 cells did not form either colonies in soft agar or tumors in vivo when 10^3 of them were transplanted. Interestingly, when 10^4 AST-L61 cells were

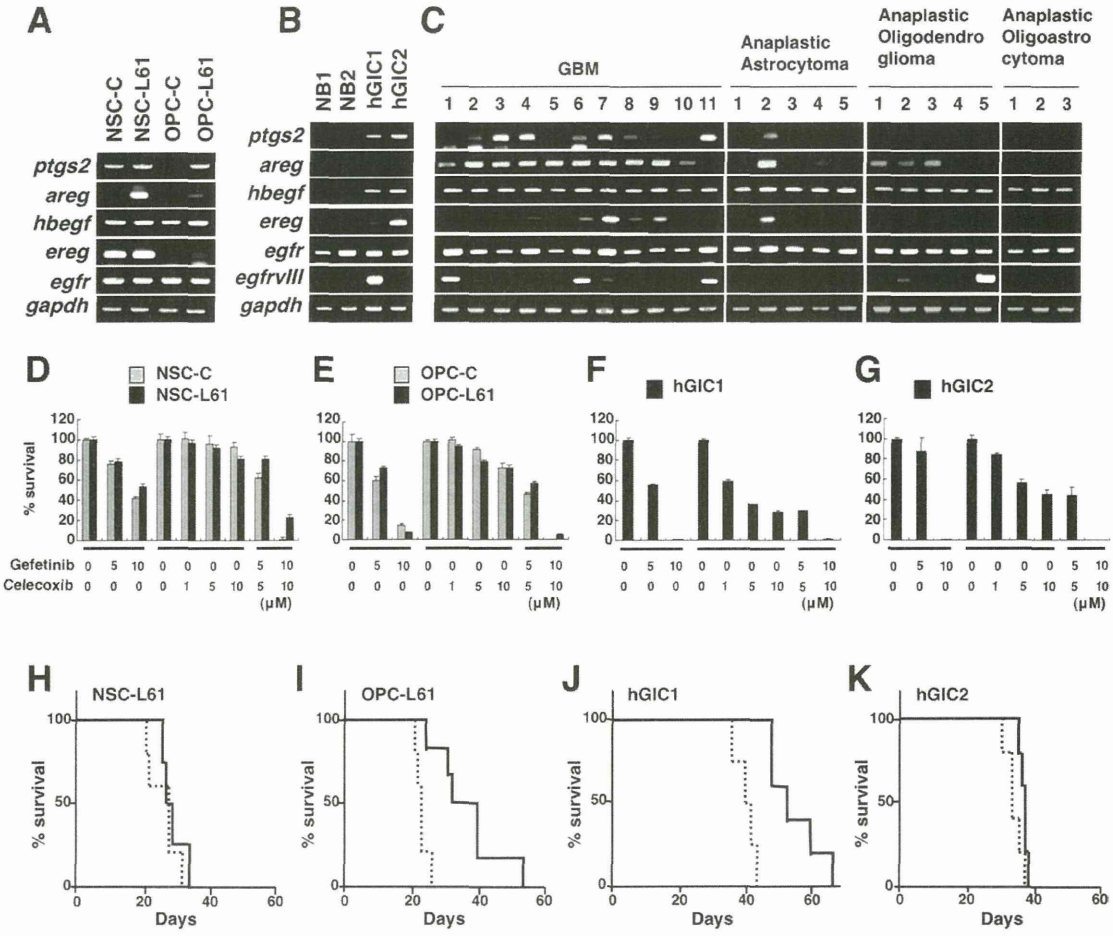

Figure 5. Combination of a Ptgs2 inhibitor and an epidermal growth factor receptor (EGFR)-signaling inhibitor delays the tumorigenesis of oligodendrocyte lineage-derived GICs. **(A–C):** Expression analysis of *ptgs2*, EGFR ligands (*areg*, *hbegf*, and *ereg*), *egfr*, and *egfrvIII* in GIC-like cells, hGICs, and human glioma samples (GBM, anaplastic astrocytoma, anaplastic oligodendroglioma, and anaplastic oligoastrocytoma), by reverse transcription polymerase chain reaction. *gapdh* expression was an internal control. **(D–G):** Cytotoxic effects of Gefitinib and Celecoxib on induced glioma cells (black column in **[D, E]**), their parental cells (gray column in **[D, E]**), hGIC1 **(F)**, and hGIC2 **(G)**. **(H–K):** Survival curve of NSC-L61- **(H)**, OPC-L61- **(I)**, hGIC1- **(J)**, or hGIC2-injected mice **(K)**, treated with the drug combination (C+G, solid line). Control mice were given water only (dotted line). Abbreviations: GBM, glioblastoma multiforme; GIC, glioma-initiating cell; hGIC, human GIC; NSC, neural stem cell; OPC, oligodendrocyte precursor cell.

transplanted into the brain of nude mice, they formed invasive astrocytoma. Theoretically, because tumors are likely to arise from one or a few CICs, AST-L61 cells are not GIC-like cells but might be premalignant cells that need additional mutation(s) to transform into GIC-like cells, or they might need a specific niche to induce tumorigenesis [36]. It will be interesting to examine which oncogenic mutations can transform astrocytes into GICs.

It has been thought that precursor cells and differentiated cells acquire characteristics of tissue-specific stem cells when they are transformed. Indeed, here we found that when OPCs were transformed into GIC-like cells, they lost their original features and acquired characteristics of NSCs. Although the detailed mechanism of the dedifferentiation caused by transformation remains to be elucidated, it is likely that epigenetic modification plays an important role, as we previously showed that epigenetic modification is involved in OPC reversion [16, 37] and that activation of the Ras-signaling pathway induces alterations in epigenetic modification, chromatin structure, and gene expression [38–42]. As OPCs can be purified and cultured in serum-free medium with defined chemicals and mitogens, OPC transformation might be a good model for investigating the molecular mechanisms of dedifferentiation in tumorigenesis.

Using GIC-like cell models, we demonstrated that oligodendrocyte lineage-derived GBMs (hGIC1) are sensitive to treatment with a Ptgs2 inhibitor and an EGFR-signaling inhibitor in combination, whereas those derived from GBM tissues (hGIC2) were not. As there is much evidence showing that chromosome 1p and 19q loss is a marker for increased sensitivity to standard therapies (chemotherapy and radiation therapy), we examined the 1p and 19q status in the two hGIC lines using the fluorescence in situ hybridization and found that hGIC2 had lost both 1p and 19q, whereas hGIC1 only lost 1p (data not shown), suggesting that the increased sensitivity to the Gefitinib/Celecoxib combination in hGIC1 was not related to the 1p/19q deletions.

There are several possible explanations for why the drug combination appeared more effective in the oligodendrocyte lineage-derived tumors than in GBM tissues. First, EGFR signaling is known to be involved in OPC proliferation and tumorigenesis [43, 44]. Second, the accumulation of Cox2-expressing astrocytes is more often observed in high-grade oligodendroglioma than in GBM [45, 46]. Third, hGIC1 and Hs683 strongly expressed egfrvIII, which was shown by Mellinghoff et al. to cause "pathway addiction" of the tumor cells [47]. Fourth, the National Cancer Institute's Repository for Molecular Brain Neoplasia Data (REMBRANDT) database [48] revealed that the downregulation of either *ptgs2* or *egfr* mRNA is correlated with a significant increase in the survival of oligodendroglioma, but not of GBM patients (Supporting Information Fig. 6). Thus, these data suggest that the combination of these inhibitors with irradiation/chemotherapy may be effective in patients suffering from oligodendrocyte lineage-derived GBMs and point to potential new clinical approaches combining current and GIC-specific therapies.

Conclusion

In this study, we have shown that induced GBM models are useful for investigating the cells-of-origin of GBM, their characteristics, and therapeutic targets, when combined with studies using hGICs and human glioma samples. Our results also suggest that the therapeutic targets for GBM are different according to the cell-of-origin of the GICs. In future studies, it will be important to find specific markers for classifying GBM according to its cell-of-origin.

Acknowledgments

We thank Martin Raff for his critical reading and helpful suggestions on the article, Douglas Sipp and Hazuki Hiraga for their critical reading, Shinichi Aizawa for the *p53*-deficient mice, and Takeya Kasukawa and Junko Nishio for performing the DNA microarray analysis. This work was supported in part by a Grant-In-Aid for Scientific Research on Priority Areas from the Ministry of Education, Culture, Sports, Science and Technology of Japan to T.K.

Disclosure of Potential Conflicts of Interest

The authors indicate no potential conflicts of interest.

References

1 Reya T, Morrison SJ, Clarke MF et al. Stem cells, cancer, and cancer stem cells. Nature 2001;414:105–111.
2 Huntly BJ, Gilliland DG. Leukaemia stem cells and the evolution of cancer-stem-cell research. Nat Rev Cancer 2005;5:311–321.
3 Krivtsov AV, Armstrong SA. MLL translocations, histone modifications and leukaemia stem-cell development. Nat Rev Cancer 2007;7:823–833.
4 Kondo T, Raff M. Oligodendrocyte precursor cells reprogrammed to become multipotential CNS stem cells. Science 2000;289:1754– 1757.
5 Laywell ED, Rackic p, Kukekov VG et al. Identification of a multipotent astrocytic stem cell in the immature and adult mouse brain. Proc Natl Acad Sci USA 2000;97:13889–13894.
6 Belachew S, Chittajallu R, Aguirre AA et al. Postnatal NG2 proteoglycan-expressing progenitor cells are intrinsically multipotent and generate functional neurons. J Cell Biol 2003;161:169–186.
7 Nunes MC, Roy NS, Keyoung HM et al. Identification and isolation of multipotential neural progenitor cells from the subcortical white matter of the adult human brain. Nat Med 2003;9:439–447.
8 Rasheed BK, McLendon RE, Herndon JE et al. Alterations of the TP53 gene in human gliomas. Cancer Res 1994;54:1324–1330.
9 Bögler O, Huang HJ, Kleihues P et al. The p53 gene and its role in human brain tumors. Glia 1995;15:308–327.
10 Cancer Genome Atlas Research Network.Comprehensive genomic characterization defines human glioblastoma genes and core pathways. Nature 2008;455:1061–1068.
11 Parsons DW, Jones S, Zhang X et al. An integrated genomic analysis of human glioblastoma multiforme. Science 2008;321:1807– 1812.
12 Jeuken J, van den Broecke C, Gijsen S et al. RAS/RAF pathway activation in gliomas: the result of copy number gains rather than activating mutations. Acta Neuropathol 2007;114:121–133.
13 Reilly KM, Loisel DA, Bronson RT et al. Nf1;Trp53 mutant mice develop glioblastoma with evidence of strain-specific effects. Nature Genet 2000;26:109–113.
14 Zhu Y, Guignard F, Zhao D et al. Early inactivation of p53 tumor suppressor gene cooperating with NF1 loss induces malignant astrocytoma. Cancer Cell 2005;8:119–130.
15 Tsukada T, Tomooka Y, Takai S et al. Enhanced proliferative potential in culture of cells from p53-deficient mice. Oncogene 1993;8:3313–3322.
16 Kondo T, Raff M. Chromatin remodeling and histone modification in the conversion of oligodendrocyte precursors to neural stem cells. Genes Dev 2004;18:2963–2972.
17 Kondo T, Raff M. The Id4 HLH protein and the timing of oligodendrocyte differentiation. EMBO J 2000;19:1998–2007.
18 Li C, Wong WH. Model-based analysis of oligonucleotide arrays: expression index computation and outlier detection. Proc Natl Acad Sci USA 2001;98:31–36.
19 Smyth GK. Linear models and empirical bayes methods for assessing differential expression in microarray experiments. Stat Appl Genet Mol Biol 2004;3:article3.
20 Storey JD. A direct approach to false discovery rates. J R Stat Soc 2004;B64(part 3):479–498.
21 Storey JD, Tibshirani R. Statistical significance for genomewide studies. Proc Natl Acad Sci USA 2003;100:9440–9445.
22 Johe KK, Hazel TG, Muller T et al. Single factors direct the differentiation of stem cells from the fetal and adult central nervous system. Genes Dev 1996;10:3129–3140.
23 Rao MS, Noble M, Mayer-Pröschel M. A tripotential glial precursor cell is present in the developing spinal cord. Proc Natl Acad Sci USA 1998;95:3996–4001.
24 Wang S, Sdrulla A, Johnson JE et al. A role for the helix-loop-helix protein Id2 in the control of oligodendrocyte development. Neuron 2001;29:603–614.
25 Bizub D, Blair D, Alvord G et al. Correlation between H-ras p21TLeu61 protein content and tumorigenicity of NIH3T3 cells. Oncogene 1988;3:443–448.
26 Kleihues P, Louis DN, Scheithauer BW et al. The WHO classification of tumors of the nervous system. J Neuropathol Exp Neurol 2002;61:215–229.
27 Singh SK, Clarke ID, Terasaki M et al. Identification of a cancer stem cell in human brain tumors. Cancer Res 2003;63:5821–5828.
28 Singh SK, Hawkins C, Clarke ID et al. Identification of human brain tumour initiating cells. Nature 2004;432:396–401.
29 Uchida N, Buck DW, He D et al. Direct isolation of human central nervous system stem cells. Proc Natl Acad Sci USA 2000;97:14720–14725.
30 Gasparini G, Longo R, Sarmiento R et al. Inhibitors of cyclo-oxygenase 2: A new class of anticancer agents? Lancet Oncol 2003;4:605–615.
31 Dancey JE. Predictive factors for epidermal growth factor receptor inhibitors—The bull's-eye hits the arrow. Cancer Cell 2004;5:411–415.
32 Yuan X, Curtin J, Xiong Y et al. Isolation of cancer stem cells from adult glioblastoma multiforme. Oncogene 2004;23:9392–9400.
33 Shinojima N, Tada K, Shiraishi S et al. Prognostic value of epidermal growth factor receptor in patients with glioblastoma multiforme. Cancer Res 2003;63:6962–6970.
34 Torrance CJ, Jackson PE, Montgomery E et al. Combinatorial chemoprevention of intestinal neoplasia. Nat Med 2000;6:1024–1028.

35 Zhang X, Chen ZG, Choe MS et al. Tumor growth inhibition by simultaneously blocking epidermal growth factor receptor and cyclooxygenase-2 in a xenograft model. Clin Cancer Res 2005;11:6261– 6269.
36 Li L, Neaves WB. Normal stem cells and cancer stem cells: The niche matters. Cancer Res 2006;66:4553–4557.
37 Lyssiotis CA, Walker J, Wu C et al. Inhibition of histone deacetylase activity induces developmental plasticity in oligodendrocyte precursor cells. Proc Natl Acad Sci USA 2007;104:14982–14987.
38 Chadee DN, Peltier CP, Davie JR. Histone H1(S)-3 phosphorylation in Ha-ras oncogene-transformed mouse fibroblasts. Oncogene 2002;21: 8397–8403.
39 Dunn KL, He S, Wark L et al. Increased genomic instability and altered chromosomal protein phosphorylation timing in HRAS-transformed mouse fibroblasts. Genes Chromosomes Cancer 2009;48: 397–409.
40 He J, Kallin EM, Tsukada Y et al. The H3K36 demethylase Jhdm1b/Kdm2b regulates cell proliferation and senescence through p15(Ink4b). Nat Struct Mol Biol 2008;15:1169–1175.
41 Agger K, Cloos PA, Rudkjaer L et al. The H3K27me3 demethylase JMJD3 contributes to the activation of the INK4A-ARF locus in response to oncogene-and stress-induced senescence. Genes Dev 2009; 23:1171–1176.
42 Barradas M, Anderton E, Acosta JC et al. Histone demethylase JMJD3 contributes to epigenetic control of INK4a/ARF by oncogenic RAS. Genes Dev 2009;23:1177–1182.
43 Aguirre A, Dupree JL, Mangin JM, Gallo V. A functional role for EGFR signaling in myelination and remyelination. Nat Neurosci 2007; 10:990–1002.
44 Ivkovic S, Canoll P, Goldman JE. Constitutive EGFR signaling in oligodendrocyte progenitors leads to diffuse hyperplasia in postnatal white matter. J Neurosci 2008;28:914–922.
45 Deininger MH, Meyermann R, Trautmann K et al. Cyclooxygenase (COX)-1 expressing macrophages/microglial cells and COX-2 expressing astrocytes accumulate during oligodendroglioma progression. Brain Res 2000;885:111–116.
46 Temel SG, Kahveci Z. Cyclooxygenase-2 expression in astrocytes and microglia in human oligodendroglioma and astrocytoma. J Mol Histol 2009;40:369–377.
47 Mellinghoff IK, Wang MY, Vivanco I et al. Molecular determinants of the response of glioblastomas to EGFR kinase inhibitors. N Engl J Med 2005;353:2012–2024.
48 Madhavan S, Zenklusen JC, Kotliarov Y et al. Rembrandt: Helping personalized medicine become a reality through integrative translational research. Mol Cancer Res 2009;7:157–167.

See www.StemCells.com for supporting information available online.